EXAMPLES OF WIDE-ANGLE WAVE-EQUATION MODELING

Bert Jacobs

Abstract

A generalized phase-shift method is used to generate one-way wave-equation models in a variable velocity medium. The small-dip and derivative approximations used in finite-difference algorithms are not employed by the new procedure.

Introduction

In the phase-shift method for solving the one-way wave-equation the wavefield at one z-level is multiplied by a phase factor to obtain the field at the next z-level. We can generalize this by decomposing the wavefield into eigenvector components. Each component may then be independently projected with an appropriate phase shift.

In generalizing phase-shift techniques so that they handle variable- velocity media, we obtain a method for generating high accuracy synthetics which can be compared with the output of more economical production programs.

Theoretical Background

Starting with the two-dimensional, monochromatic, constant density wave equation, we take appropriate Fourier transforms and discretize the transformed wave equation. The discretization leads to an eigenvalue problem for a Hermitian matrix. The eigenvalues and eigenvectors will be used in projecting the wavefield from z-level to z-level.

The wave equation is

$$\frac{\partial^2}{\partial x^2} u(x,z,\omega) + \frac{\partial^2}{\partial z^2} u(x,z,\omega) + \frac{\omega^2}{v^2(x,z)} u(x,z,\omega) = 0 \qquad (1)$$

With Fourier transform definitions

$$A(\omega) = \frac{1}{\sqrt{(2\pi)}} \int_0^\infty dt\ a(t)\, e^{i\omega t}$$

$$B(p_x) = \frac{1}{\sqrt{(2\pi)}} \int_{-\infty}^\infty dx\ b(x)\, e^{-ip_x x}$$

$$C(p_z) = \frac{1}{\sqrt{(2\pi)}} \int_0^\infty dz\ c(z)\, e^{-ip_z z}$$

an upgoing wave will be of the form $e^{i\omega t + p_z z}$ if p_z and ω take the same sign.

Taking Fourier transforms over all variables in equation 1 we get

$$W(p_x,z) = \frac{1}{\sqrt{(2\pi)}} \int_{-\infty}^\infty dx\ v^{-2}(x,z)\, e^{-ip_x x} \tag{2}$$

$$-p_z^2\, u(p_x,z,\omega) + \frac{\omega^2}{\sqrt{(2\pi)}} \int_{-\infty}^\infty dp_x'\ W(p_x - p_x',z)\, u(p_x',z,\omega) = p_z^2\, u(p_x,z,\omega) \tag{3}$$

The discretization of equation 3 will be easier if we define two $n_x\ x\ n_x$ matrices, $\hat{W}$ and $\hat{D}$. $\hat{W}$ is highly structured - it is an $n_x\ x\ n_x$, Hermitian, Toeplitz, and circulant matrix (where n_x is the number of grid points along the x-axis). Since it is circulant, $\hat{W}$ is completely determined by its top row. Letting N subscript the Nyquist wavenumber for the x-direction, the top row of $\hat{W}$ is given by

$$\left[W_0\ W_1\ W_2 \cdots\ W_{N-1}\ W_N\ W_{N-1}^* \cdots\ W_2^*\ W_1^*\right]$$

$\hat{D}$ is defined by

$$\hat{D} = diag\left[0\ 1\ 4\ 9 \cdots\ (N-1)^2\ N^2\ (N-1)^2 \cdots\ 9\ 4\ 1\right]$$

With these two matrices, equation 3 can be discretized

$$\left[\frac{\omega^2 \Delta p_x}{\sqrt{(2\pi)}}\, \hat{W} - \left[\Delta p_x\right]^2 \hat{D}\right] U = p_z^2\, U \tag{4}$$

where

$$U^T = \left[u_0\, u_1\, u_2 \cdots\ u_{2N-1}\right]$$

$$\Delta p_x = \frac{2\pi}{n_x \Delta x}$$

Equation 4 has a nontrivial solution only when p_z is an eigenvalue and U is an eigenvector. There are $2N$ eigenvalue-eigenvector pairs which we can index with λ.

This poses a problem because it is extremely unlikely that our upgoing wave will be an eigenvector of the wave-equation matrix in equation 4. We get around this by decomposing the wavefield $U(x,z,\omega)$ into eigenvector components $\varphi_\lambda(x,z,\omega)$, where it is understood that x,z, and ω will from now on be taken to be discrete variables. The decomposition is defined by the two equations

$$c_\lambda = \sum_{x=0}^{2N-1} \varphi_\lambda^*(x,z,\omega)\, U(x,z,\omega) \tag{5}$$

$$U(x,z,\omega) = \sum_{\lambda=0} c_\lambda \varphi_\lambda(x,z,\omega) \tag{6}$$

All that is left now is to figure out how to extrapolate U. This is easy since we know how to extrapolate the eigenvectors. We propose to use

$$\varphi_\lambda(x,z-\Delta z,\omega) = \varphi_\lambda(x,z,\omega)\, e^{i\, sgn(\omega)\, |p_{z\lambda}|\, \Delta z} \qquad (p_{z\lambda}\ real) \tag{7}$$

If $p_{z\lambda}$ is imaginary then we can pick its sign so that the wave field decays in the extrapolation direction or we can set c_λ=0. In our program we will do the latter.

Algorithm

If we wished to extrapolate a monochromatic wavefield we would start at positive z and move towards the surface. At any given z-level, the first thing to do is to add the contribution of the exploding reflector sources to the wavefield $U(x,z,\omega)$. The eigenvalue problem must be solve for the matrix in equation 4. With the eigenvectors from this step, we decompose the wavefield according to equation 5. Each component is extrapolated with equation 7 and the extrapolated components recombined, as in equation 6.

This process can be repeated over a range of discrete frequencies to get the frequency domain representation of the synthetic. Fourier transforming over ω generates the synthetic.

Examples

The generalized phase shift algorithm was coded up and tested to explore the characteristics of its output. The first synthetic is the seismogram due to a buried source in a constant velocity medium. The grid parameters of the input were $nx=32$, $nz=32$, $dx=5.0$, and $dz=5.0$. If (ix,iz) is used to describe the position of a point in the x,z-plane using Cartesian coordinates, then unit sources were placed at (24,16) and (25,16). The velocity of the medium was set equal to 1000. The time axis in the output space has 32 samples and the sampling rate was 0.005.

The synthetic exhibits the usual hyperbola with the usual (and undesirable) wraparound in both the t- and x-directions. Some high-frequency noise

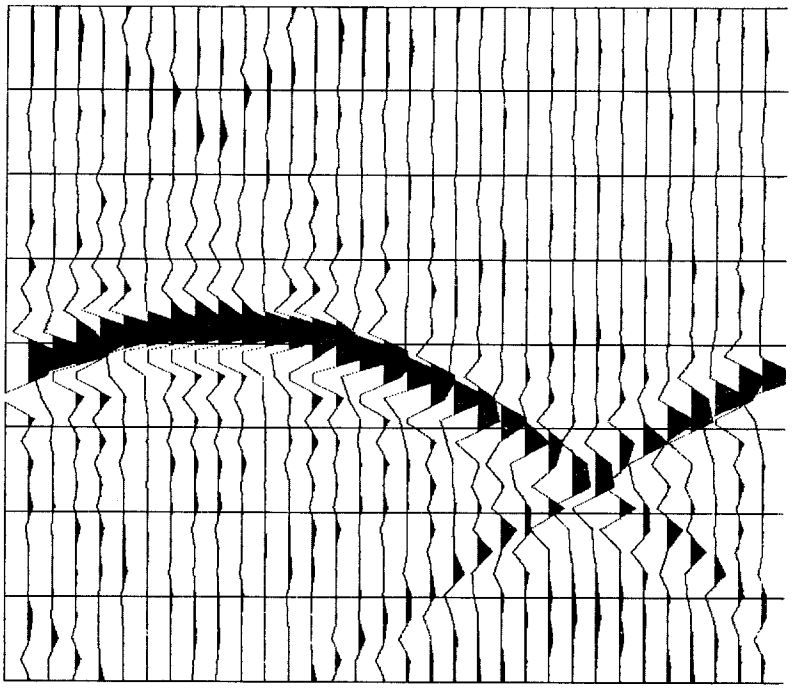

FIG. 1. A constant velocity model generated by the generalized phase-shift method. The timing lines are 0.02 seconds apart.

is evident on the plot of the output. This chatter is probably due to roundoff errors.

A variable velocity model was attempted next. With the same discretization parameters as that of the constant velocity model, unit sources were placed at (12,16), (13,16), (21,16), and (22,16). The velocity was set equal to 1000 to the left of the

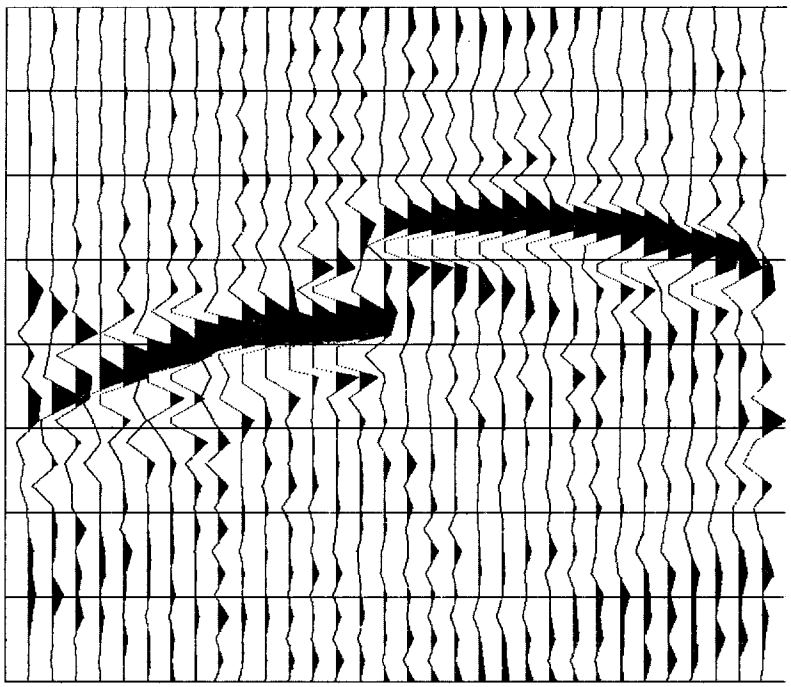

FIG. 2. Variable velocity modeling with the phase-shift method. Reflections from the velocity discontinuities at the sides and middle of the section are prominent.

17th grid point on the x-axis and equal to 1500 to the right of that grid point. Thus, the hyperbola on the right is both flatter and earlier than the one on the left. The rest of the synthetic
looks noisy because of roundoff, wraparound, and reflections from the velocity discontinuities. Due to the periodicity of the Fourier transform, there are an infinite number of interfaces from which our upgoing wave bounces. These reflections add considerably to the incoherent appearance of the output sections.

Smoothing the velocity discontinuities should reduce the reflections due to variable velocity distributions. The third model is the same as the second except that an anti-aliasing filter was applied to the slowness squared distribution at each z-step. This had a desirable effect of reducing the reflections from the model's velocity gradients. It had the undesirable effect of generating a resonance in the vicinity of one of the velocity jumps. One hypothesis for this effect is that the resonance is taking place between the Gibb's effect peaks created by the anti-aliasing filter.

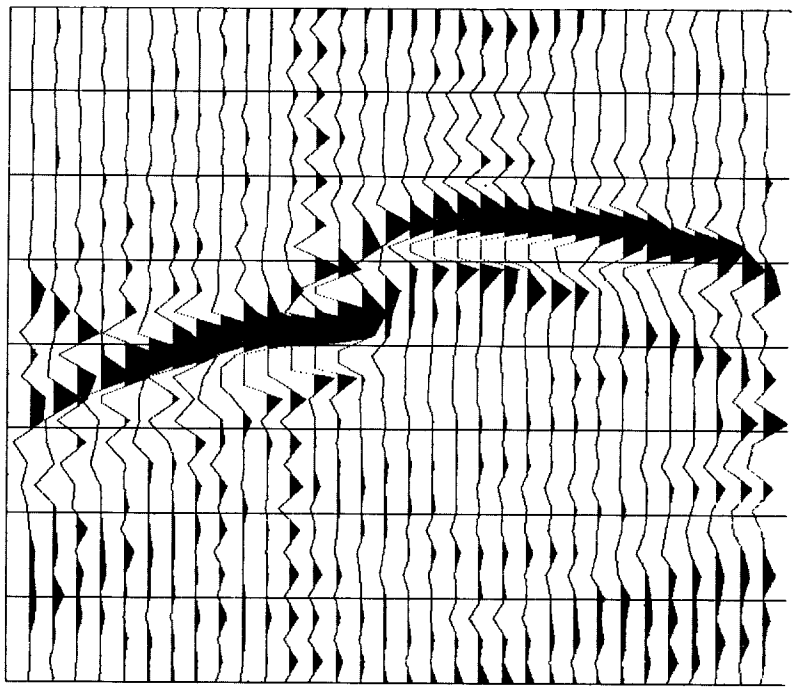

FIG. 3. Variable velocity synthetic due to a model very similar to that of Figure 2. An anti-aliasing filter was applied to the series sampling the square of the material slowness. Note the resonance at the interface.